Supplementary Information

For

Lattice-Matched Molecular-Anchor Design for High-Performance Perovskite Quantum Dot Light-Emitting Diodes

Jiawei Chen[1,2,+], Xiangyu Liu[1,+], Bo Cai[3,+], Yuanzhuang Cheng[1], Hao Wen[4], Danlei Zhu[1], Yaonan Xiong[5], Linjie Dai[6], Xinghua Yan[1], Baixu Xiang[4], Xiyu Luo[1], Wenjing Feng[1], Jiuyao Du[1], Shuyue Dong[1], Qingsong Shan[2], Shulin Chen[5], Haibo Zeng[2], Qihua Xiong[4], Lian Duan[1,7] & Dongxin Ma[1,7]**

This file contains:

Supplementary Figures 1 – 12

Supplementary Tables 1 – 2

Supplementary References 1 – 11

Supplementary Fig. 1 | Crystal models of $CsPbI_3$ for DFT calculation. a, $CsPbI_3$ with trap defects. b, $CsPbI_3$ treated with the single-site molecule. c, $CsPbI_3$ with lattice-matched multi-site anchoring effect. 3

Supplementary Fig. 2 | The PLQY distribution of QD solution treated with different molecules. The error bars represent the highest and lowest PLQYs while the boxes represent the average PLQYs. 4

Supplementary Fig. 3 | The ultrafast differential transmission spectra at room temperature. a, pristine QDs. b, target QDs. The photon energy of pump beam is ~ 2.14 eV. The pump fluence is ~ 0.61uJ/cm^{-2}. 5

Supplementary Fig. 4 | SEM images of $CsPbI_3$ QD films. a, The control QD film. b, The target QD film. Scale bars, 500 nm. 6

Supplementary Fig. 5 | AFM images of $CsPbI_3$ QD films. a, The control QD film. b, The target QD film. Scale bars, 400 nm. 7

Supplementary Fig. 6 | EL performance of the control and target QLEDs. a, Luminance-voltage curves. b, Luminance-EQE curves. c, Radiance-EQE curves. 8

Supplementary Fig. 7 | Performance of target QLEDs with different concentrations of TMeOPPO-*p* in ethyl acetate. a, 5 mg mL^{-1}. b, 7.5 mg mL^{-1}. c, 10 mg mL^{-1}. 9

Supplementary Fig. 8 | Accelerated ageing tests for QLED at different R_0. a, The control device. b, The target device. 10

Supplementary Fig. 9 | The relation between luminance and radiance of the typical green perovskite LEDs. a, Current density-voltage curves. b, EQE curves. c, EL spectrum, with peak locating at 520 nm and FWHM of 20 nm. d, Radiance versus driving voltage characteristics. e, Luminance-voltage curves. f, The ratio of the value of radiance to the value of luminance. 11

Supplementary Fig. 10 | The performance of the typical QLED with low roll-off. a, Current density versus voltage curve. b, Radiance versus driving voltage characteristics. c, EQE versus current density curve. 12

Supplementary Fig. 11 | Summary of the reported iodine-based perovskite QLED characteristics (600~800 nm). 13

Supplementary Fig. 12 | Accelerated ageing tests for the QLEDs with various molecules. a, TPPO, b, TMeOPPO-*o*, c, TFPPO. d, TClPPO. e,TBrPPO. 14

Supplementary Table 1 | PL lifetime of the pristine and target perovskite QD films .. 15

Supplementary Table 2 | Summary of the typical reported perovskite QLEDs (600~800 nm) 16

Supplementary References 17

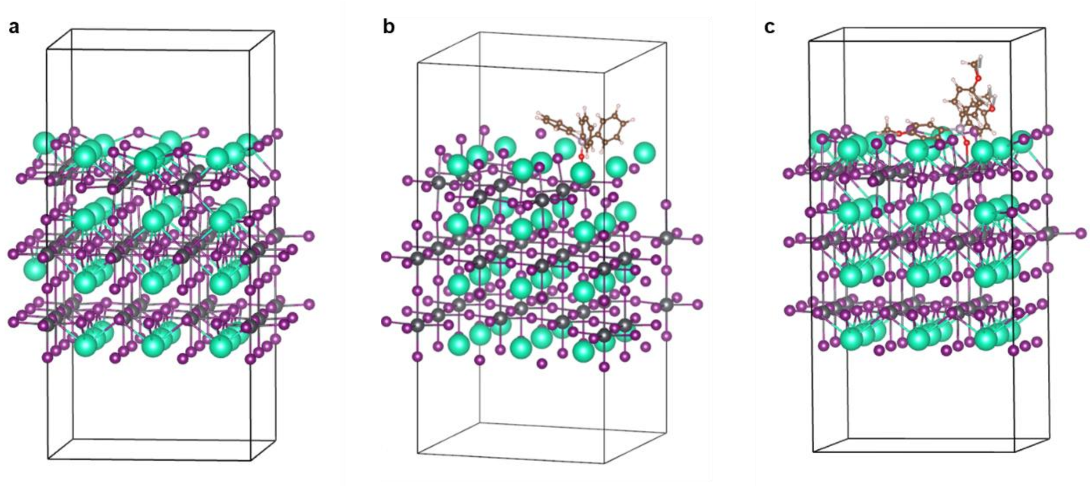

Supplementary Fig. 1 | Crystal models of $CsPbI_3$ for DFT calculation. **a**, $CsPbI_3$ with trap defects. **b**, $CsPbI_3$ treated with the single-site molecule. **c**, $CsPbI_3$ with lattice-matched multi-site anchoring effect.

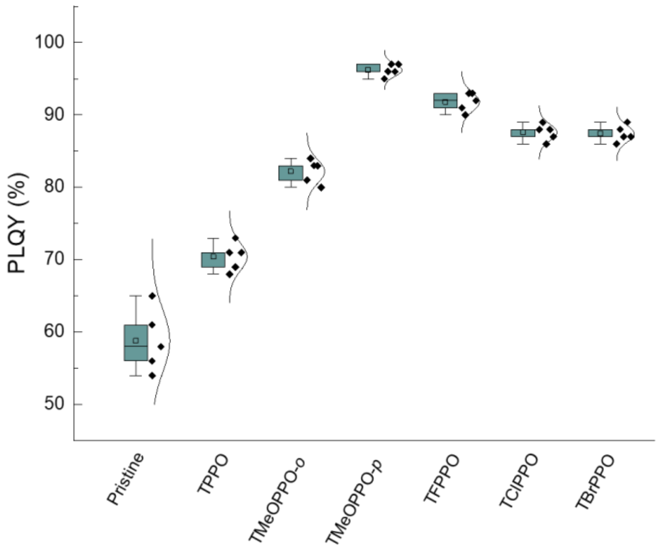

Supplementary Fig. 2 | The PLQY distribution of QD solution treated with different molecules. The error bars represent the highest and lowest PLQYs, while the boxes represent the average PLQYs.

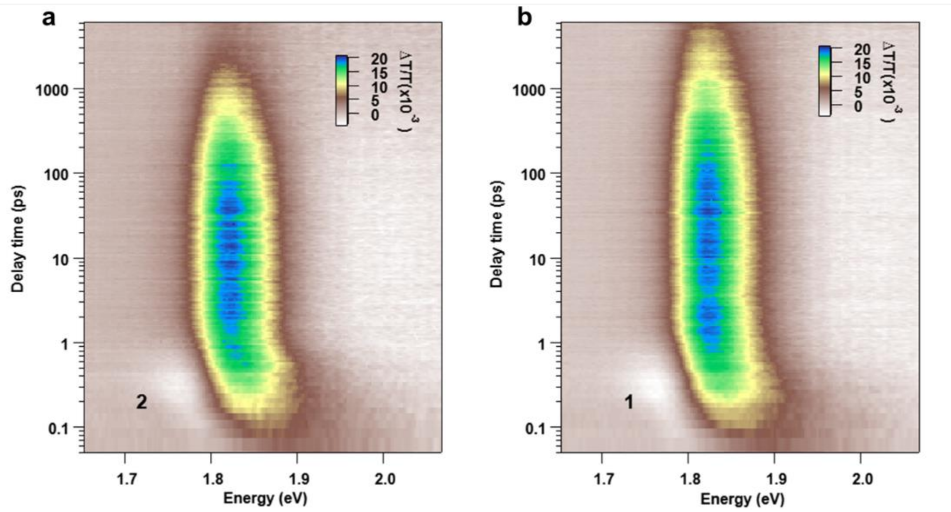

Supplementary Fig. 3 | The ultrafast differential transmission spectra at room temperature. a, pristine QDs. **b**, target QDs. The photon energy of pump beam is ~ 2.14 eV. The pump fluence is ~ 0.61uJ/cm^{-2}.

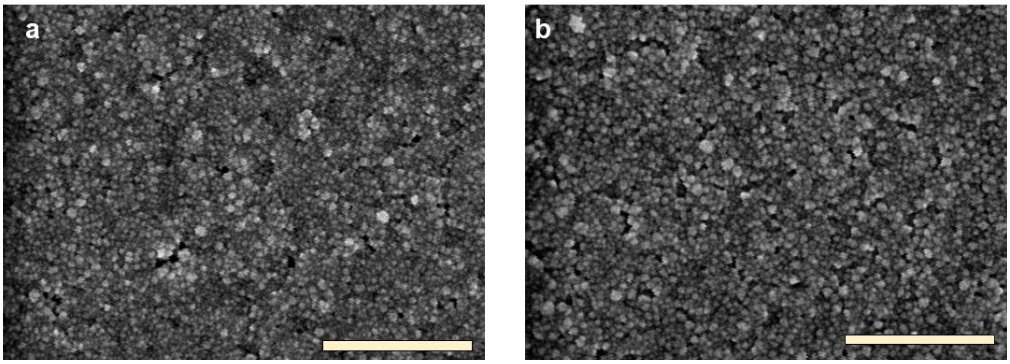

Supplementary Fig. 4 | SEM images of $CsPbI_3$ QD films. a, The control QD film. **b**, The target QD film. Scale bars, 500 nm.

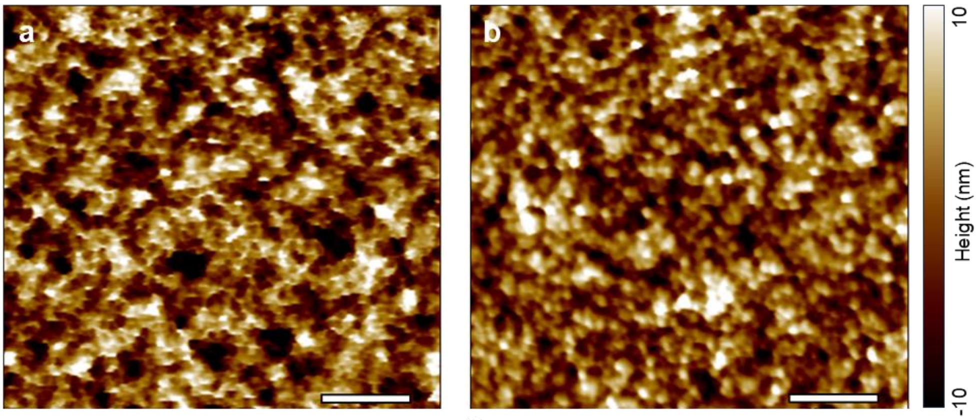

Supplementary Fig. 5 | AFM images of $CsPbI_3$ QD films. a, The control QD film. **b**, The target QD film. Scale bars, 400 nm.

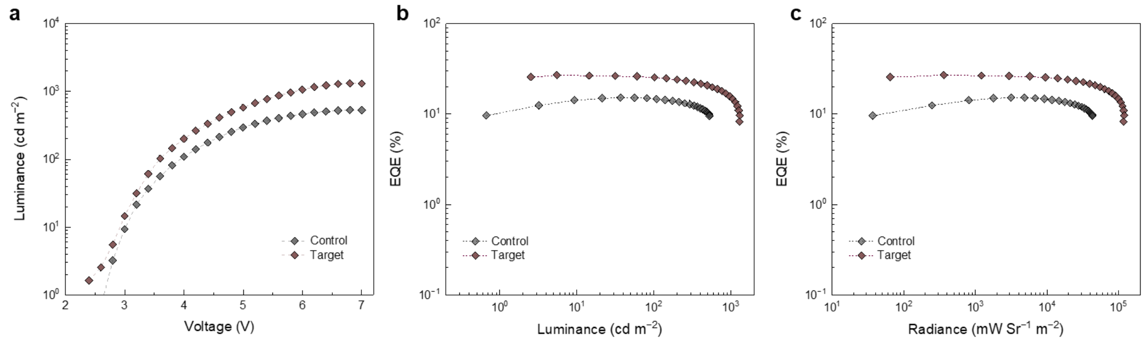

Supplementary Fig. 6 | EL performance of the control and target QLEDs. a, Luminance-voltage curves. **b**, Luminance-EQE curves. **c**, Radiance-EQE curves.

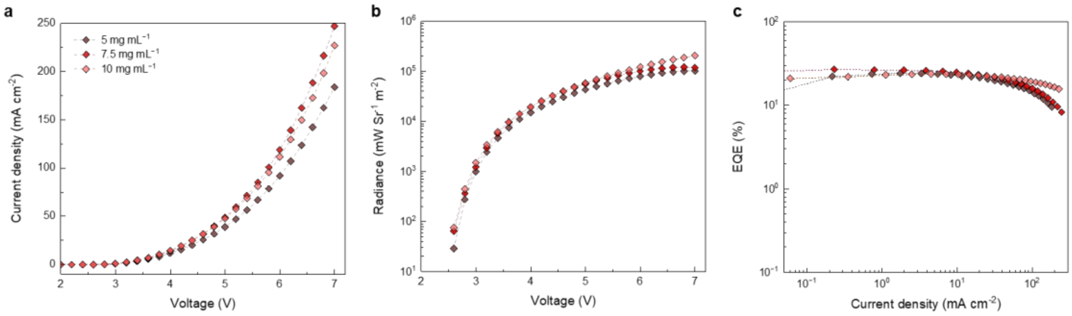

Supplementary Fig. 7 | Performance of target QLEDs with different concentrations of TMeOPPO-*p* in ethyl acetate. a, 5 mg mL^{-1}. **b**, 7.5 mg mL^{-1}. **c**, 10 mg mL^{-1}.

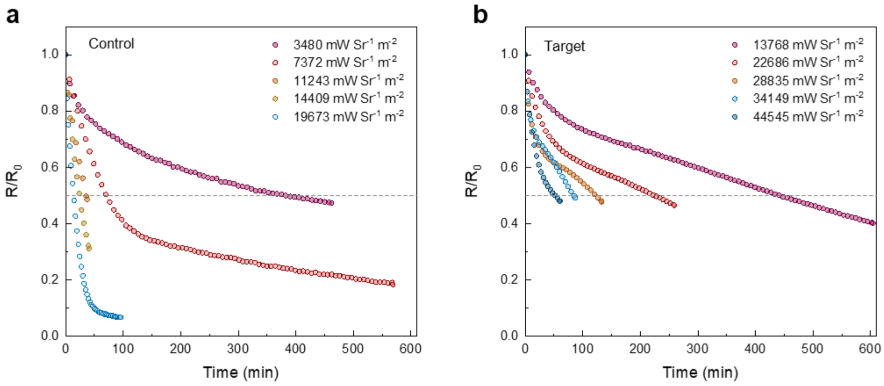

Supplementary Fig. 8 | Accelerated ageing tests for QLED at different R_0. a, The control device. **b**, The target device.

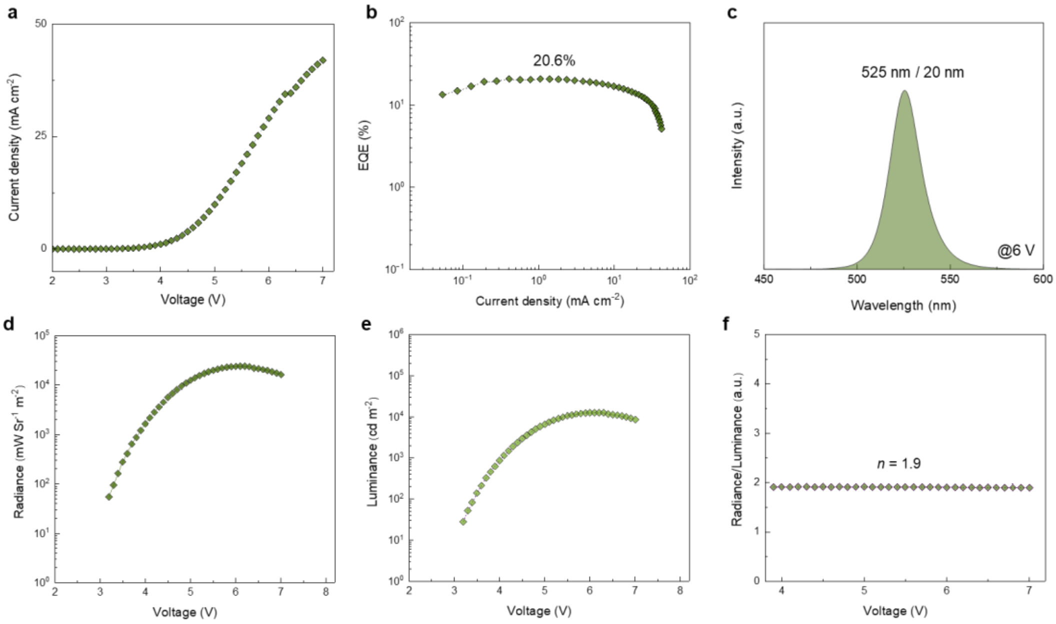

Supplementary Fig. 9 | The relation between luminance and radiance of the typical green perovskite LEDs. a, Current density-voltage curves. **b,** EQE curves. **c**, EL spectrum, with peak locating at 520 nm and FWHM of 20 nm. **d,** Radiance versus driving voltage characteristics. **e,** Luminance-voltage curves. **f,** The ratio of the value of radiance to the value of luminance.

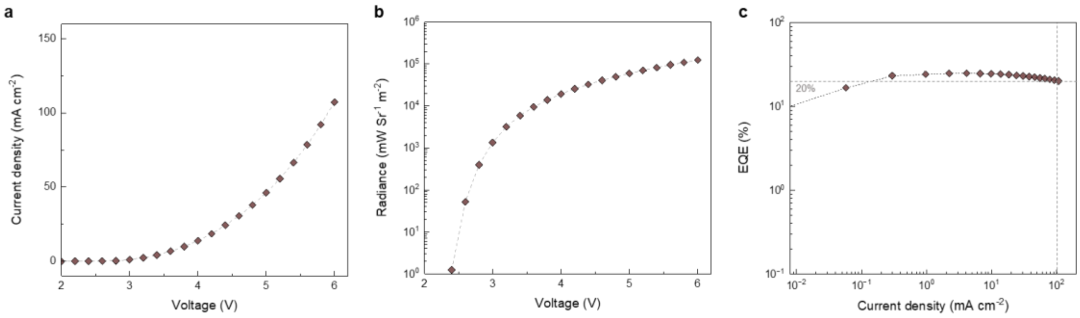

Supplementary Fig. 10 | The performance of the typical QLED with low roll-off. a, Current density versus voltage curve. **b**, Radiance versus driving voltage characteristics. **c**, EQE versus current density curve.

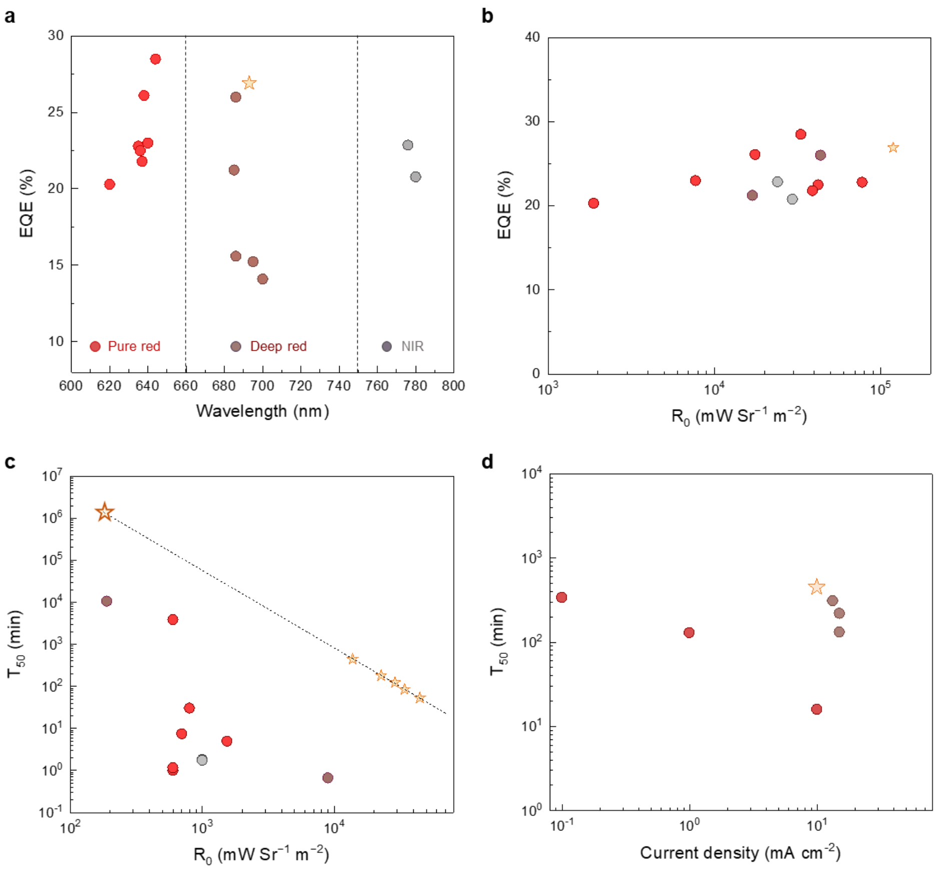

Supplementary Fig. 11 | Summary of the reported iodine-based perovskite QLED characteristics (600~800 nm).

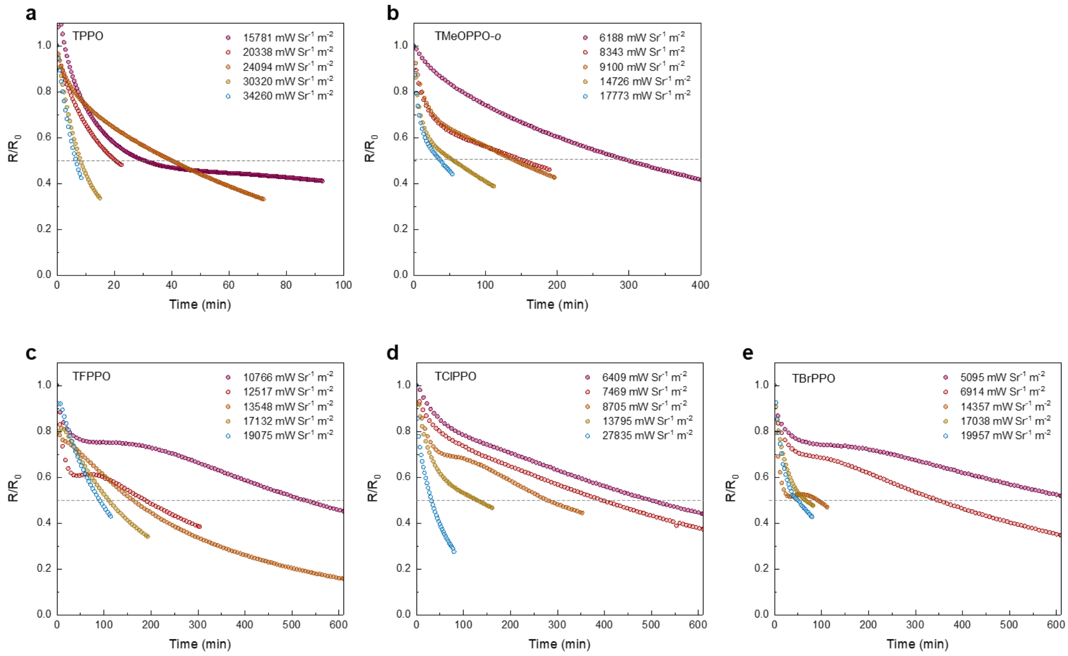

Supplementary Fig. 12 | Accelerated ageing tests for the QLEDs with various molecules. a, TPPO, **b**, TMeOPPO-*o*, **c**, TFPPO. **d**, TClPPO. **e**,TBrPPO.

Supplementary Table 1 | PL lifetime of the pristine and target perovskite QD films

	Pristine	Target
A_1	0.67	0.37
τ_1	2.97	3.60
A_2	0.30	0.57
τ_2	20.77	31.29
τ_{avg}	8.22	19.17
R^2	0.997	0.998

Supplementary Table 2 | Summary of the typical reported perovskite QLEDs (600~800 nm)

QD	EL Peak (nm)	EQE (%)	L_{max}/R_{max} (cd m^{-2}/mW sr^{-1} m^{-2})	T_{50} (h)	Condition*	Ref.
$MAPb(Br/I)_3$	620	20.3	627/~1,880	2.17	1 mA cm^{-2}	1
				0.27	10 mA cm^{-2}	
$CsPb(Br/I)_3$	635	22.8	12,910/~77,460	1	100 cd m^{-2}/~600 mW sr^{-1} m^{-2}	2
$CsPbI_3$	636	~22.5	7,000/~42,000	~3,900	100 cd m^{-2}/~600 mW sr^{-1} m^{-2}	3
$CsPb(Br/I)_3$	637	21.8	6,471/~38,946	1.17	100 cd m^{-2}/~600 mW sr^{-1} m^{-2}	4
$CsPb(Cl/I)_3$	638	26.1	2,511/~17,577	7.5	100 cd m^{-2}/~700 mW sr^{-1} m^{-2}	5
$CsPbI_3$	640	23	~1000/7,700	5	200 cd m^{-2}/~1540 mW sr^{-1} m^{-2}	6
				5.67	0.1 mA cm^{-2}	
$CsPbI_3$	644	28.5	4,140/~33,120	30.4	100 cd m^{-2}/~800 mW sr^{-1} m^{-2}	7
$CsPbI_3$	685	21.23	190/~17,000	0.67	100 cd m^{-2}/~9000 mW sr^{-1} m^{-2}	8
$CsPbI_3$	686	26.0	492/43,691	10,587	190 mW sr^{-1} m^{-2}	9
				5.17	13.3 mA cm^{-2}	
$FAPbI_3$	776	22.86	NA/24,000	1.83	1000 mW sr^{-1} m^{-2}	10
$FAPbI_3$	780	20.79	NA/29,470	1.75	1000 mW sr^{-1} m^{-2}	11
$CsPbI_3$	693	26.91	1,305/119,037	23,420	190 mW sr^{-1} m^{-2}	This work
				7.43	10 mA cm^{-2}	

*Radiance is estimated by testing as-fabricated perovskite QLED with the corresponding EL peak.

Supplementary References

1 Hassan, Y. *et al.* Ligand-engineered bandgap stability in mixed-halide perovskite LEDs. *Nature* **591**, 72-77 (2021).

2 Zhang, J. *et al.* Ligand-Induced Cation–π Interactions Enable High-Efficiency, Bright, and Spectrally Stable Rec. 2020 Pure-Red Perovskite Light-Emitting Diodes. *Adv. Mater.* **35** (2023).

3 Wang, Y. K. *et al.* Long-range order enabled stability in quantum dot light-emitting diodes. *Nature* (2024).

4 Xie, M. *et al.* Suppressing Ion Migration of Mixed-Halide Perovskite Quantum Dots for High Efficiency Pure-Red Light-Emitting Diodes. *Adv. Funct. Mater.* (2023).

5 Feng, Y. *et al.* Nucleophilic Reaction-Enabled Chloride Modification on CsPbI3 Quantum Dots for Pure Red Light-Emitting Diodes with Efficiency Exceeding 26 %. *Angew. Chem. Int. Ed.* **63**, e202318777 (2024).

6 Wang, Y. K. *et al.* All-Inorganic Quantum-Dot LEDs Based on a Phase-Stabilized alpha-CsPbI(3) Perovskite. *Angew. Chem. Int. Ed.* **60**, 16164-16170 (2021).

7 Li, H. *et al.* Nanosurface-reconstructed perovskite for highly efficient and stable active-matrix light-emitting diode display. *Nat. Nanotechnol.* **19**, 638-645 (2024).

8 Cheng, H. *et al.* Size Enlargement of CsPbI3 Perovskite Nanocrystals by Trioctylphosphine in the Synthesis for Highly Efficient Deep-Red Light-Emitting Diodes. *Adv. Electron. Mater.*, 2400334 (2024).

9 Chen, J. *et al.* Molecule-induced ripening control in perovskite quantum dots for efficient and stable light-emitting diodes. *Sci. Adv.*, eado7159 (2025).

10 Liu, Z. S. *et al.* Liquid bidentate ligand for full ligand coverage towards efficient near-infrared perovskite quantum dot LEDs. *Light: Science & Applications* **14**,

35 (2025).

11 Wang, Y. *et al.* Ligand-Solvent Coordination Enables Comprehensive Trap Passivation for Efficient Near-Infrared Quantum Dot Light-Emitting Diodes. *Angew. Chem. Int. Ed.* **63**, e202407833 (2024).